



## 1 INTRODUCTION

In recent decades, the automotive industry has experienced considerable technological development, according to a demand for more and more challenging. Today, due to the globalization car manufacturers are innovating every day, in a sense of growing competition in the market by introducing vehicles more comfortable, safe, economic and environmentally friendly throughout.

In this way the choice of materials became an important step in the eco-conception, which can contribute significantly in environment preservation. Composite materials with organic matrix can be good alternative to replacement of classical metallic materials. During the last century, the introduction of advanced composite materials in various industries (aerospace, aerospace, automotive ...) was a striking success. The strengths of these materials reside in: their lightness, their chemical stability and their implementation facilities.

However, the physical properties of these materials vary depending on several factors: the nature of the matrix and the reinforcement, the architecture and the reinforcement rate ... etc. In an economic context the use of mid-range materials is preferred in automotive mass production. In this context, the thermoplastic matrix based composites reinforced with glass fiber are good candidates. Recyclability of thermoplastics is one of their various advantages. In addition, these materials are characterized by their low density which gives a considerable lightness in comparison to metallic materials. This significant weight saving has a direct impact on the surrounding, by the considerable decrease of emission of non-desirable gases such as (CO<sub>2</sub>).

One of these materials materials that are used increasingly in automotive field is polyamide-6 (PA-6), which is a semi crystalline polymer characterized by acceptable mechanical properties, good resistance to fatigue, chemicals and hydrocarbons. However, it has poor resistance to water and its implementation requires drying [1]. The use of this material as matrix constitutes an ideal candidate for the manufacture of thermoplastic composites reinforced with glass fibers for the automotive industry.

However, at thickness and shape equivalent composite materials based on PA-6 reinforced with glass fibers are not equivalent to steels in terms of overall rigidity.

In order to overcome this difficulty, a new technique of composite manufacture has been developed; this technique is composite over-molding.

This study is made in the framework of FUI project ARIZONA, which consists in a new methodology of composite manufacturing from thermoplastic prepreg combined with injected composite based on PA6 matrix

The objective of this work is to characterize thermal-mechanical and mechanical properties of different zones of the composite part: laminate, injected and over-molded zones in relation with the processing parameters and moisture content.

## 2 MATERIALS & METHODES

### 2.1 Materials

The materials used in this study were three Polyamide PA6 based composites:

- Continuous glass fibers reinforced PA6, commercially named Tepex Dynalyte 102 RG 600(2); the reinforcement of this material is a balanced fabric with 0° and 90° oriented made from two plies of 0.5 mm oriented at [0°, 90°] given a total thickness of 1mm. The reference of the material in this study is CGFR-PA6. Fiber weight fraction is about 64% (cf. fig.1.1).

- Injected composite reinforced by discontinuous glass fibers with a nominal length of 250 $\mu$ m; this material is made with the same grade of PA6 and commercially named Durethan BKV 60 characterized by fiber weight fraction of 62% (cf. fig.1.2). The reference of the material in this study is DGFR-PA6.
- Over-molded composite which is a bi-layered composite between continuous and discontinuous fiber reinforced composite.

All materials were supplied by Bond-Laminates GmbH<sup>®</sup> and Lanxess<sup>®</sup>.

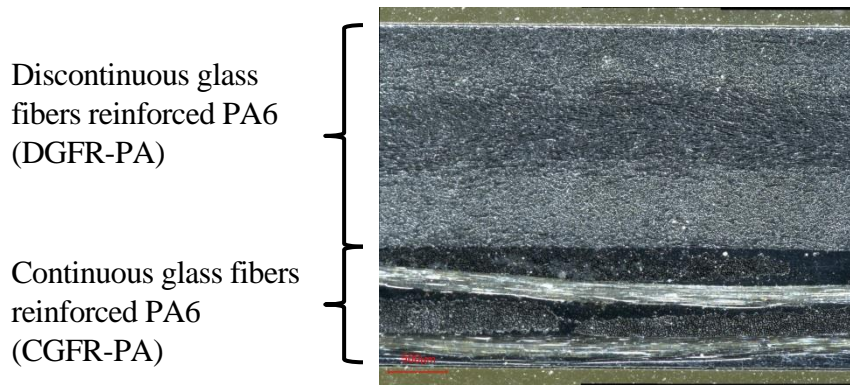


Fig.1. Numerical optical micrograph showing over-molded composite layers.

In the aim to characterize the effect of process manufacturing parameters, a prototype part with a complex shape was designed in ARIZONA project. The design was carried out by Mecaplast<sup>®</sup> after shape optimization given by LTDS. The mold was realized by Compose<sup>®</sup>. All prototype parts were manufactured at the PEP<sup>®</sup>. The prepreg lay-up was consolidated as a plate, pre-heated with an IR heating system, and put inside the mold. The plate was then thermoformed by closing the mold and over-molded by injecting the DGFR-PA6 (Fig.1.b) in one step.

Temperature of pre-heating was varied as follow: 250, 270, 285 and 295°C. Mold temperature was 110°C.

All specimens were obtained by water jet cutting from prototypes.

## 2.2 Thermomechanical analysis

Rheological characteristics of materials were performed with the use of DMA50 0.1dB from METRAVIB on rectangular (20mm $\times$ 2mm $\times$  thickness mm) specimens in the tension/compression mode at controlled alternating strain. The temperature range was -130°C to 200°C with a heating rate of 1°C/min and the frequency was varied from 0.1 to 30 Hz.

## 2.3 Tree point bending test

The three point bending loadings were carried out using an INSTRON 4206 electromechanical machine with load cells of 100 kN and cross head speed was 2.5 mm/min. The radius of the load roller was 5 mm and the distance between supports was 60 mm. Experimental procedure was made according to the International standard ISO 14125 at room temperature ( $T=23\pm 1^\circ\text{C}$ ,  $\text{RH} = 40\pm 5\%$ ). CGFR-PA6 samples have the following dimensions: 100 mm long, 25 mm wide and 1 mm thick. In the case of DGFR-PA6 and over-molded composite the samples dimensions are 100 mm long, 15 mm wide and 3 mm thick.

The apparent flexural elastic modulus ( $E_f$ ) and the ultimate stress ( $\sigma_{\max}$ ) were the mechanical properties evaluated.

Figure (fig.2) shows an example of three point bending curves of DGFR-PA6 composite. The linear part corresponds to the elastic behavior and the maximum recorded stress is considered as an ultimate flexural stress.

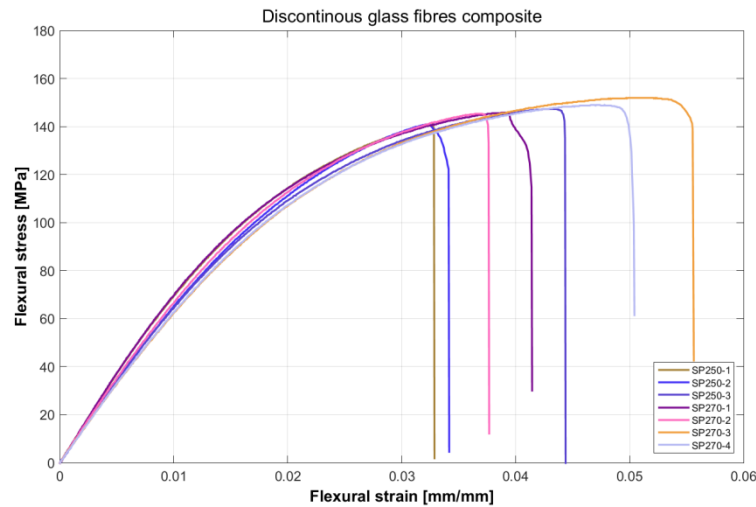


Fig.2. Flexural stress vs flexural strain curve (three bonding test): Discontinuous glass reinforced PA6.

## 2.4 Computed tomography analysis

The computed tomography is a non-destructive method based in the 3D X ray scan which allows three-dimensional structure information of materials without contact. The micro-tomograph used is Nanotm<sup>®</sup> research edition manufactured by General Eclectic inspection Technology. It allows analysis of samples size: height from 1 mm to 120 mm, maximum 100 mm width and sample acquisition in aqueous medium. The X-ray source is an open tube GE Phoenix nano-focus, providing a maximum voltage of 180 kV and a maximum power of 15 W. The voltage range operates between 10 and 180 kV. The apparatus detector is a digital detector with dimensions 115 mm x 115 mm, with a pixel size of 50 microns x 50 microns (2300 x 2300 matrix px). It provides submicron resolution (minimum pixel size of 0.5 microns). However the pixel resolution is highly dependent on the specimen size.

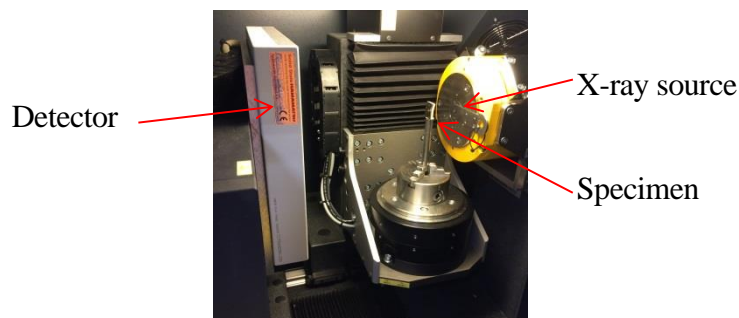


Fig.3. Micro-tomography device.

The test parameters used in this study are as follows: sample dimensions 15 mm long, 15 mm width and 4 mm thick and the beam operated at 80 keV and 120  $\mu$ A. According to the sample size the voxel resolution achieved in this study was 8  $\mu$ m. The result obtained by X-ray tomography was a stack of slices in 3 directions which includes about 2400 images. These slices were analysed using VG-studio and ImageJ to generate 3D representation of the specimens.

### 3 RESULTS & DISCUSSIONS

#### 3.1 Materials conditioning

Effect of moisture content on PA6 based composite on mechanical properties were investigated. Specimens were dried for 8 days in stove at 60°C, in the objective to remove all residual moisture due to air conditioning and transportation. After surface polishing of sample the absorption of water was achieved by immersion in distilled water at room temperature ( $T = 23^\circ\text{C} \pm 2^\circ\text{C}$ ). Uptake moisture of specimens was measured by differential weighting using an electronic balance of accuracy  $10^{-5}$  g. Difference between the weight of dried specimens and the weight after water immersion was calculated. Supposing that in the composite only the matrix PA6 uptakes water, the moisture content  $M(t)$  absorbed by each specimen was calculated from its initial weight ( $w_0$ ) of dried matrix PA6 and its weight after absorption ( $w_t$ ) as follows:

$$w_0 = w_{0c} \cdot (1 - X_f) \quad (\text{eq.1})$$

$$w_t = w_{tc} - w_{0c} \quad (\text{eq.2})$$

Where, ( $w_{0c}$ ) is the initial weight of the composite, ( $X_f$ ) is the weight fraction of the fiber (0.64%) and ( $w_{tc}$ ) the weight of conditioned composite at the instant  $t$ .

$$M(t) = 100 \cdot \left( \frac{w_t - w_0}{w_0} \right) \quad (\text{eq.3})$$

Figure VI.1 shows the weight gain  $M(t)$  as a function of the square root of time ( $t^{1/2}$ ) during ageing in distilled water for the studied composites. Three specimens were studied for each case and the presented water uptakes are average values.

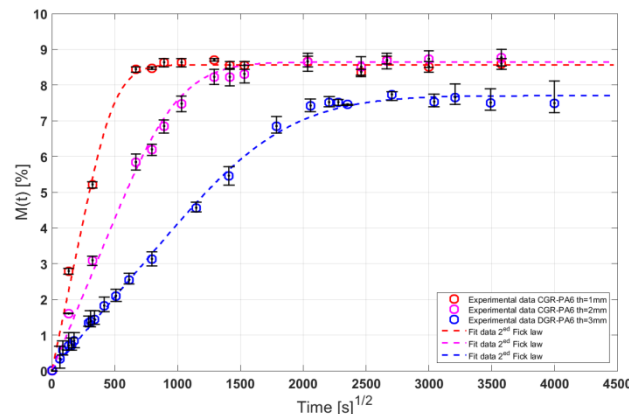


Fig.4. Moisture content evolution as a function of time for the three composites CGFR-PA6 1 mm thick, CGFR-PA6 2 mm thick and CGFR-PA6 3 mm thick

All composite curves showed similar profiles and one can distinguish the presence of two zones. The first one is linear corresponding to a rapid increase of moisture content. The second region corresponds to a plateau at which the aged material reaches saturation. In this case, and for all studied composites the kinetics of water diffusion follow the one-dimensional Fick's second law. The coefficient of diffusion of water can be calculated from the slope ( $S$ ) of the linear part of the last curves as follows [2]:

$$D = \pi \left( \frac{h}{4M_\infty} \right)^2 (S)^2 \quad (\text{eq.4})$$

By considering the coefficients  $D$  and  $M_m$ , the moisture content as a function of time  $M(t)$  can be expressed according to the following equation [3]:

$$\frac{M(t)}{M_\infty} = 1 - \sum_{n=0}^{\infty} \frac{8}{\pi^2(2n+1)^2} \exp\left(-\frac{D(2n+1)^2\pi^2 t}{h^2}\right) \quad (\text{eq.5})$$

where  $M_\infty$  is the moisture content at saturation,  $D$  is the apparent diffusion coefficient,  $t$  is the aging time and  $h$  is the sample thickness.

The apparent diffusion coefficient and the maximum moisture content vary with the nature of composite. The continuous glass reinforced PA-6 composites achieved moisture saturation at 8.7% with an apparent coefficient of water diffusion equal to  $7.01 \text{ e-}7 \text{ mm}^2/\text{s}$  whereas the discontinuous glass reinforced PA-6 composite (DGFR-PA6) showed better hygrothermal properties since the water diffusivity and the moisture content at saturation were lower than for the CGFR-PA6 ( $M_\infty = 7.7\%$  and  $D= 5.1 \text{ e-}7 \text{ mm}^2/\text{s}$ ).

### 3.2 Dynamical mechanical analysis

The storage moduli ( $E'$ ) and the loss factor ( $\tan \delta$ ) as a function of the temperature and frequency for all composites were measured by DMA.

In order to determine different relaxation temperatures, CPGR-PA6 composite were oriented at  $\pm 45^\circ$  according to the direction of loading. Figure 3 shows an example of the evolution of storage modulus ( $E'$ ) and damping factor ( $\tan(\delta)$ ) as a function of temperature and frequency for CPGR-PA6. These figures compare two moisture content states: dried and wet at saturation.

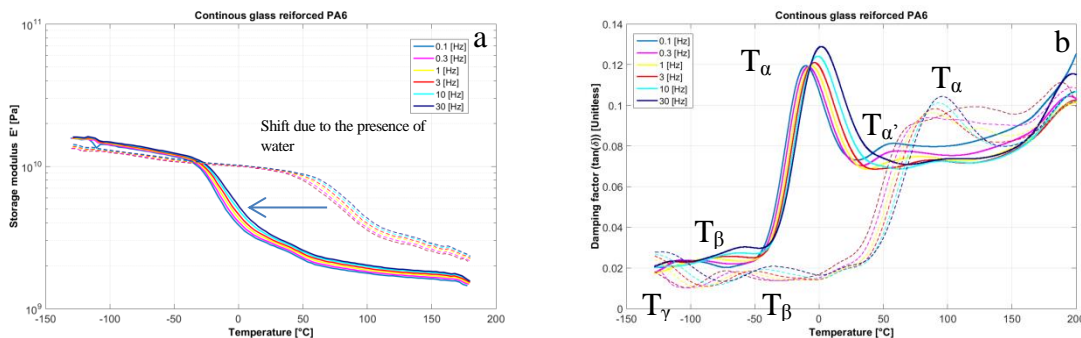


Fig. 5. Evolution of viscoelastic properties of CGFR-PA6 oriented at  $\pm 45^\circ$  measured by DMA as versus temperature and frequency : a) Storage modulus  $E'$  b) damping factor ( $\tan(\delta)$ ).  
(----) dried composite (—) wet composite.

In the range of temperature studied ( $-130 - 200 \text{ }^\circ\text{C}$ ) a decrease of storage modulus is observed with temperature increase. The structural change occurring in polymeric materials is a result of the molecular mobility at different time scales. These motions are known as molecular relaxations. In the case of dried composites three clear relaxations can be distinguished:

- the main relaxation or relaxation- $\alpha$  corresponding to the drastically decrease of the storage modulus and the highest peak of the  $\tan(\delta)$ ; this relaxation is associated to the glass transition, and corresponds to the coordinated motion of relatively long chain segments by debonding of low energy bonds (hydrogen bonds) [4]. This relaxation occurs approximately at  $T_\alpha = 80 - 90^\circ\text{C}$  depending on frequency.
- two sub- $T_g$  relaxations [5-6]: the relaxation- $\beta$  and relaxation- $\gamma$  corresponding to the motions of small chain segments or molecular functions. The relaxation- $\beta$  involves the rotation of the amide functions and occurs in the range of  $-80 / -40^\circ\text{C}$  approximately; the

relaxation-  $\gamma$  corresponds to the vibrational motions of the methylene functions in the chains and it occurs at around  $-130^{\circ}\text{C}$ .

After conditioning the composites by water immersion, the DMA results show that the presence of water in the PA6 matrix involves a shift of mechanical molecular relaxations to low temperature as observed in fig.5. In fact, the  $T_{\alpha}$  decreases from  $80^{\circ}\text{C}$  in dried composite to  $-10^{\circ}\text{C}$  for wet composite at 1Hz as shown in Figure (fig.6).

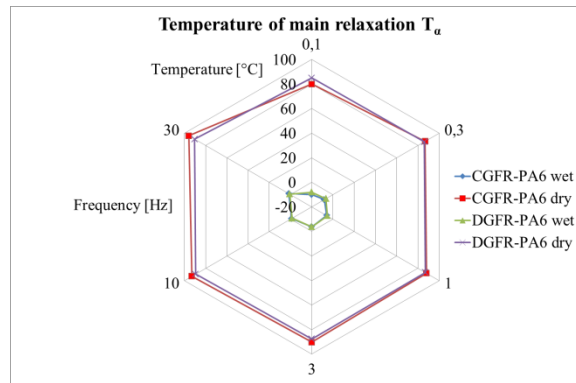


Fig.6. Temperature of main relaxation versus moisture content for different loading frequencies.

In the case of the main relaxation ( $\alpha$ ) the shift of temperature is due to the fact that the presence of water increases the local volume by separating the polymer chains [11, 12].

### 3.3 Three-point bending tests

Mechanical properties of all composites according to the process conditions and moisture content were studied using 3-point bending test. The apparent flexural modulus was taken as a main mechanical property discriminant between different composites.

Figures (fig.7.a & fig.7.b) compare the flexural properties of Continuous GFR-PA6 and Discontinuous GFR-PA6 respectively for different processing conditions and sampling zones. Prepreg heating was varied from 250 to 295  $^{\circ}\text{C}$ . In all cases the composite failure occurred on the tensile side.

The results show there is not a significant variation in the apparent flexural modulus for the two composites whatever the processing conditions. Nevertheless there is a large modulus range for discontinuous fiber reinforced composite (7-16 GPa) due to the fiber architecture which varies with sampling zone.

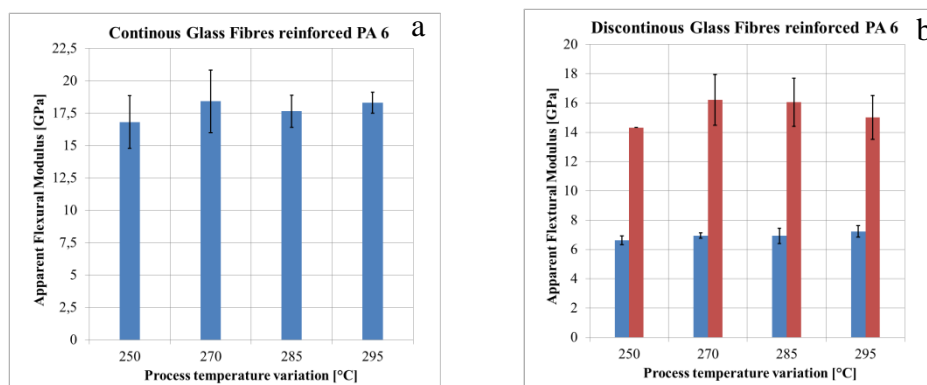


Fig.7. Evolution of apparent flexural modulus according to the temperature process variation: a) CGFR-PA6 and b) DGFR-PA6 (zone1 blue & 2 red).

Figures (Fig.8.a & Fig.8.b) compare the flexural properties of over-molded composites for different processing temperatures. Due to the multi-layering feature of these composites, two bending configurations were investigated: in the first, continuous glass fibers on tensile side and in the second on compressive side.

Fig.8.a and Fig.8.b show the homogenized apparent flexural modulus and the ultimate flexural strength respectively.

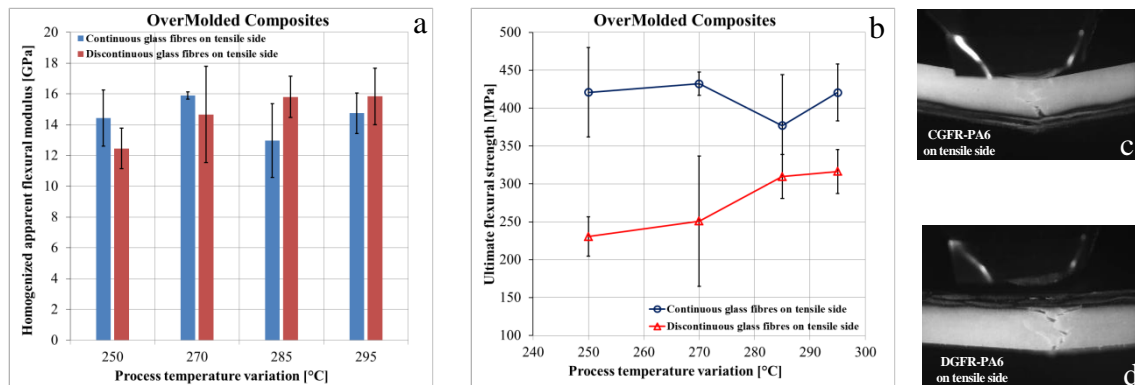


Fig.8. Evolution of flexural properties for the over-molded composite: a) apparent flexural modulus b) Ultimate flexural strength c) and d) illustration of different bending configurations and failure features.

The results show that there is no clear tendency concerning the apparent flexural modulus according to the temperature processing and bending configuration. This behavior is probably associated to the complex fiber architecture according to sampling zone (fig.8.a). The ultimate flexural strength evolution according to the different mode of bending is shown in figure (fig.8.b). When the CGFR-PA6 is on the tensile side the flexural strength is the highest and quasi-stable whatever the processing conditions. For the system with the discontinuous fibers on the tensile side the ultimate stress increases with the processing conditions probably due to a better interface between the two composites. The computed tomography technique was used to investigate failure mode of the over-molded systems. Fig.9 shows an example of 3D reconstitution computed from X-ray slices for continuous glass fibers on the tensile side (Fig.9.a) and discontinuous glass fibers on the tensile side (Fig.9.b). These figures show typical failure features. In the case when CGFR-PA6 is on the tensile side the failure grows through the two composites (Fig.9.a). However, in the second case (discontinuous fibers on the tensile mode) the failure occurs through the discontinuous glass fiber composite and at the interface between the two materials (Fig.9.b).

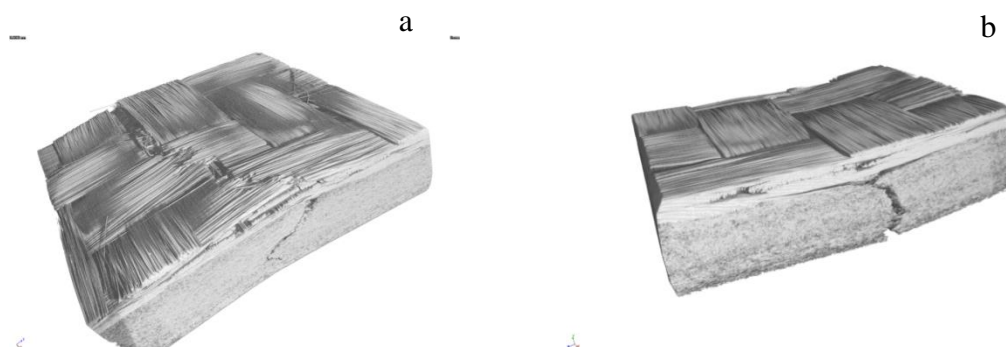


Fig.9. 3D micro-tomography representation of over molded composite after 3-point bending test: a) CGFR-A6 on the tensile side and b) DGFR-A6 on the tensile side.



This analysis confirms that the scattering of the results is due to the fiber architecture of the injected composite. In fact, the injection flow makes the fiber orientation: in some cases the skin/core morphology is dominant with high thickness of skin layer and with fibers oriented principally in longitudinal direction, leading to a higher strength. Figure (fig.10) shows two over-molded composites with the same process parameters but presenting different ultimate flexural strength (a :  $\sigma_{max} = 190$  MPa, b:  $\sigma_{max} = 312$  MPa).

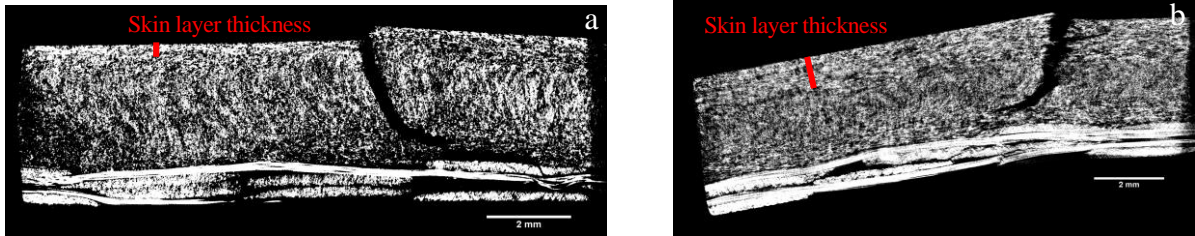


Fig.10. Micro-tomography slices showing discontinuous fibers orientation for the same process conditions but different sampling zones.

*Effect of moisture on flexural properties*

Figure (fig.11) illustrates the evolution of apparent flexural modulus (fig.11.a) and ultimate flexural strength (fig.11.b) as a function of moisture content for all studied composites for a given sampling zone.

The results show a sharp decrease in the flexural modulus as well as in the ultimate flexural strength. The continuous glass fibres reinforced PA6 observes a decrease of 50% in apparent flexural modulus and the ultimate flexural strength for the moisture saturation state. At 5% of moisture content the decrease of flexural modulus is about 50% and the flexural strength was reduced of about 36%.

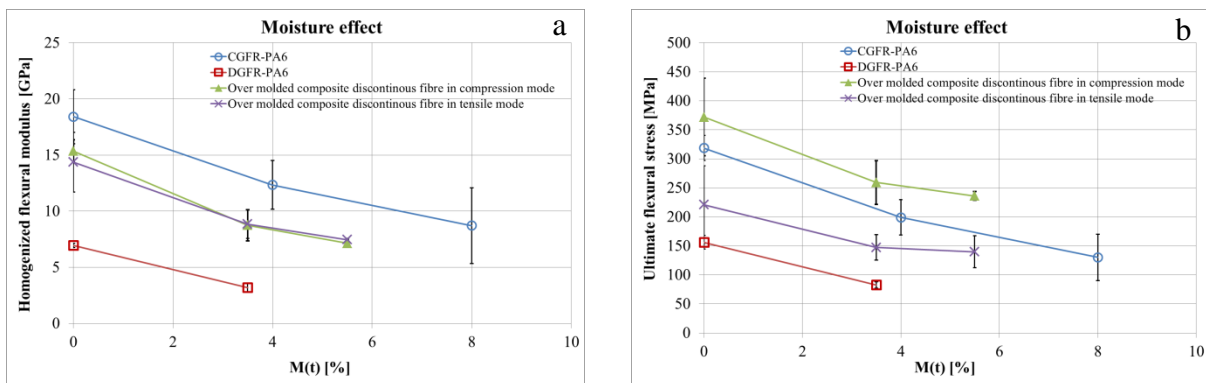


Fig.11. Evolution of flexural properties according to the moisture content for all composites: a) Apparent flexural modulus and b) ultimate flexural stress.

As shown previously with DMA, the absorbed water decreases the main relaxation of PA6 due to the plasticizing action of water molecules. This phenomenon leads to a drop of the modulus of the matrix at room temperature, and therefore to a decrease of the composite one (mixture law). Moreover, the increase in molecular mobility of the wet matrix reduces the yield stress and increases the ductility and elongation at break of the composite.

## 4 CONCLUDING REMARKS

In this study the thermomechanical and mechanical properties of PA6 composites was investigated. This work demonstrates that the conditioning history and environment conditions are important parameters to be taken into account in design of structural part composites based on PA6. The PA6 matrix is very sensitive to humidity; the sorption of water can decrease drastically the thermal and mechanical properties of glass fiber reinforced PA6 composites. The over-molding of prepreg composite can be a solution to enhance the rigidity and therefore the mechanical properties of composite parts by a local addition of discontinuous glass fiber reinforced composite.

## 5 ACKNOWLEDGEMENTS

The authors would like to acknowledge all the partners of ARIZONA project, Guillaume Huguet from Mecaplast®, Mathieu Schwander from PEP®, Guillaume Salaun from Compose® and Jean-Marie Olive from Lanxess® and our colleagues in ECL for their help: Jerome Laborde, Jean-Michel Vernet and Benoit Ponsard.

## 6 REFERENCES

- [1] L. Monson, M. Braunwarth, and C.W Extrand, Moisture absorption by various polyamides and their associated dimensional changes, *Journal of Applied Polymer Science*, (107): 355-363, .2008.
- [2] C.H. SHEN, G.S. SPRINGER, Moisture Absorption and Desorption of Composite Materials, *Journal of Composite Materials*, (10) : 2-20, 1976
- [3] W. Jost, Diffusion in Solids, Liquids, Gases. New York: Academic Press, 1960.
- [4] A. Owen, R. Bonart, Cooperative relaxation processes in polymers, *Polymer*, (26):1034, 1985.
- [5] Y. Park, J. Ko, T-K. Ahn, and S. Choe, Moisture Effects on the Glass Transition and the Low Temperature Relaxations in Semiaromatic Polyamides, *J. Polym. Sci. Part B: Polym. Phys.*, (35): 807, 1997.
- [6] G. Rotter and H. Ishida, Dynamic Mechanical Analysis of the Glass Transition: Curve Resolving Applied to Polymers, *Macromolecules*, (25): 2170, 1992.
- [7] N.S. Murthy, Hydrogen Bonding, Mobility, and Structural Transitions in Aliphatic Polyamides, *J. Polym. Sci. Part B: Polym. Phys.*, (44):1763, 2006.
- [8] S. Rastogi, A.E. Terry, and E. Vinken, Dissolution of Hydrogen-Bonded Polymers in Water: A Study of Nylon-4,6, *Macromolecules*, (37): 8825, 2004.
- [9] E. Vinken, A.E. Terry, O. van Asselen, A.B. Spoelstra, R. Graf, and S. Rastogi, Role of superheated water in the dissolution and perturbation of hydrogen bonding in the crystalline lattice of polyamide 4,6, *Langmuir*, 24, 6313 (2008).
- [10] Abacha et al. – eXPRESS Polymer Letters, (3) 4 : 245–255, 2009.
- [11] N. S. Murthy, M. K. Akkapedi, Analysis of lamellar structure in semicrystalline polymers by studying the absorption of water and ethylene glycole in nylons small angle neutron scattering, *Mocromelecules*, (3): 142-152, 1998.

[12] A. Bergeret, L. Ferry, P. Ienny. Vieillessement hygrothermique des composites thermoplastiques renforcés par des fibres de verre, *Revue des composites et des matériaux avancés*, (18)1: 33-49, 2008.

### **COPYRIGHT NOTICE**

Copyright ©2015 by the authors. Distribution of all material contained in this paper is permitted under the terms of the Creative Commons license Attribution-NonCommercial-NoDerivatives 4.0 International (CC-by-nc-nd 4.0).

